FOG WATER COLLECTION AND REFORESTATION AT A MOUNTAIN LOCATION IN A WESTERN MEDITERRANEAN BASIN REGION: AIR-MASS ORIGINS AND SYNOPTIC ANALYSIS

José A. Valiente, María J. Estrela, David Corell, David Fuentes, Alejandro Valdecantos and Manuel J. Baeza

With 14 figures and 3 tables
Received 02. November 2010 · Accepted 08. June 2011

Summary: An inland mountainous location in eastern Spain was selected for reforestation studies based on the fog water collection potential prevailing in the area and the high level of land degradation resulting from recurrent forest fires in the past. Bulk fog-water catches were stored and used in a micro-irrigation network to provide summer emergency water pulses to a plot of reforestation seedlings. Results indicate that survival rates and seedling growth of the two species planted, *Pinus pinaster* and *Quercus ilex*, improved with the use of small timely waterings and additional treatments with composted biosolids. Fog collection measurements during the 3-year period of the experiment revealed an average water yield of 3.2 l/m²/day, which, although moderate, is a suitable value for afforestation activities. Fog formation is explained in terms of air mass origin and pathway, atmospheric conditions and orographic features. Statistical analysis of the winds bearing fog and the periodicity of fog collection provide the particular characteristics of the experimental site.

Zusammenfassung: Die vorliegende Studie beschreibt einen Aufforstungsversuch in einer im östlichen Spanien gelegenen Gebirgsregion. Der Untersuchungsraum ist durch Landschaftsdeagradation und duch wiederholte Waldbrandereignisse in der Vergangenheit gekennzeichnet. Ziel der Studie war es zu untersuchen, ob eine gezielte Bewässerung mit gesammeltem Nebelwasser zu einer Verbesserung der Überlebenschanchen von Keimlingen und Jungpfanzen beitragen kann. Es wurden Nebelwasser-Auffangbecken angelegt und das Wasser über ein Mikro-Bewässerungsnetzwerk während sommerlicher Trockenphasen zu den Jungpflanzen geleitet. Die Ergebnisse zeigen, dass sich die Überlebenschancen von zwei der gepflanzten Arten (*Pinus pinaster* und *Quercus ilex*) durch diese gezielten Wassergaben und zusätzliche Zufuhr von Klärschlamm deutlich verbesserten. Im Mittel des dreijährigen Betrachtungszeitraums lag die Menge des gesammelten Nebelwassers bei 3,2 l/m²/Tag. Diese eigentlich eher moderaten Mengen haben sich als ausreichend für die gezielte Bewässerung erwiesen. Die Nebelbildung wird vor dem Hintergrund der Luftmassenherkunft, den atmosphärischen Bedingungen und den orographischen Verhältnissen beleuchtet und die statistische Analyse der nebelbringenden Winde und der Periodizität der gesammelten Nebelniederschläge verdeutlicht die besonderen Charakteristika des Untersuchungsraums.

Keywords: Fog collection and formation, Valencia region, reforestation, air-mass trajectory

1 Introduction

The application of assisted watering in reforestation actions is a recommended tool in arid and semiarid areas (Allen 1995; Lovich and Bainbridge 1999; Bainbridge 2002), where severe and prolonged water deficit is a common feature and precipitation has an irregular and frequently unpredictable nature. This regime of water deficit often leads to huge mortality rates in newly planted seedlings. Under dry conditions, it has been determined that periods of 120 consecutive days (or even periods of 70 or 80 days) without any significant rainfall event higher than 5 mm result in high mortality rates for Mediterranean woody species seedlings during their first summer in the field (Vallejo et al. 2000). Drought periods of 80 days are not uncommon at our restoration location (Tab. 1), even though summer precipitations may not be particularly scarce for a specific year. Moreover, these prolonged drought periods can be brought to a close by a very intense precipitation episode before the end of summer, as often occurs in Mediterranean climates. Under these circumstances, the application of water pulses during the reforestation process can improve the overall success of the restoration, and the water used can

DOI: 10.3112/erdkunde.2011.03.05 ISSN 0014-0015 http://www.erdkunde.uni-bonn.de

Tab. 1: Summer (mid-June to mid-September) rainfall and the maximum number of consecutive summer days without significant precipitation events (>5 mm) in Ayora Municipality (13 km away from the afforestation site)

Year	Summer rainfall (mm)	Drought period (days)
2005	63	36
2006	63	87
2007	34	82
2008	12	77
2009	96	34

come from a resource as interesting as fog. A one-year survey of fog water collection and its use in applying emergency water pulses deeply into the seedling root system has already been provided by Estrela et al. (2009). The present study from the same site reports the three-year results of this plantation experiment. Definite efficiencies of the application of small water pulses and nutrient-rich composted sewage sludge can now be provided by looking at the 3-year seedling survival and plant growth data. In addition, more complete fog water collection statistics can also be given for this prolonged period, revealing certain characteristics that have been observed for the winds bearing fog and for the occurrence times of fog-water collection. Furthermore, the origin of the air masses leading to fog collection at the reforestation site is also evaluated through back-trajectory analysis. A combination of trajectories and weather charts is used to describe the process through which fog could be formed and collected.

The fog water collection potential in the Valencia region, eastern Spain, has been quantified at several mountain locations (Fig. 1) (Millán et al. 1998; Estrela et al. 2004; Valiente et al. 2007; Estrela et al. 2008). These surveys are based on the use of a passive cylindrical device with a protective cover on top, which makes its fog collection efficiency independent of wind direction. On this kind of collector, fog-water collection takes place when clouds form and make contact with the surface, rendering either fog alone or a combination of fog and rainfall. For mountain sites in the Valencia region, winter and summer are characterized by frequent fog-only events, while during autumn and spring, mixed fog and rain events are more common. The latter phenomena can also be called horizontal precipitation, i.e., the wind-driven horizontally-transported component of precipitation together with the horizontally transported fog (Villegas et al. 2008). Henceforth, we will use the term "fog collection" to refer to all the water actually collected by the passive fog collector, i.e., the water generated by both situations of horizontal precipitation and fog episodes alone.

2 Study area, data and methods

2.1 Site description

Located on the western side of the Mediterranean basin, the Valencia region (Fig. 1) is situated at about the centre of the arch formed by the east coast of the Iberian Peninsula. The region is characterized by a very complex topography: narrow coastal plains that broaden at the central part of the region and high terrain inland or near the coast with their associated valleys. The presence of cliffs and ridges with at least a 500-m drop to the ground is common along the coastline, and differences in height of 300–400 m between mountain tops and valley floors are not unusual inland. The highest inland peak is Peñagolosa at 1815 m a.s.l., located in the northern part of the region 40 km from the coastline. The second highest peak (Aitana, 1558 m a.s.l.) is situated in the southern part at 15 km from the coast.

The experimental site selected for the reforestation study, Mount Los Machos, is located in the interior of the Valencia region (Fig. 1) at 60 km from the nearest coastline. This site shows appropriate topographic conditions for the development of fog events, according to the criteria laid out by Schemenauer and Cereceda (1994). The annual pluviometric regime in the whole area ranges from 400 to 600 mm, corresponding to a dry Mediterranean climate (Peñarrocha 1994). In 1979, the area experienced a large wildfire which burned 30 000 ha of mixed mature pine forest mainly dominated by maritime pine (*Pinus pinaster*) and, to a lesser extent, Aleppo pine (*P. halepensis*). The potential vegetation of the area is a sclerophyllous oak forest of *Quercus ilex* (*Bupleuro*

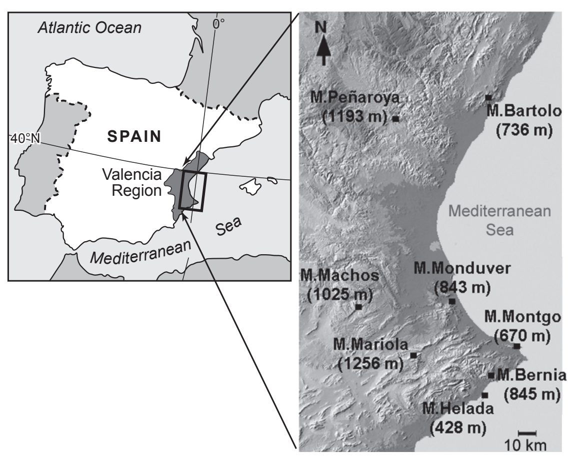

Fig. 1: Map location for the experimental site at Mount Los Machos and the other stations that use cylindrical collectors

rigidi-Quercetum rotundifoliae in RIVAS-MARTINEZ 1987), although the pre-fire vegetation was a managed mature forest. The natural post-fire vegetation dynamics led to shrublands with different degrees of development and a composition of species dominated by obligate seeders: *Ulex parviflorus*, *Rosmarinus officinalis* and *Cistus albidus* (BAEZA et al. 2007). The dominance of this new shrubland layer resulted in the accumulation of fine-fuel components, thus increasing the fire risk to a very high level (BAEZA et al. 2006). Once this naturally regenerated shrubland has fulfilled its role of protecting the soil from erosion and degradation and improving the microclimatic conditions, these communities may arrest the progression of the succession and require external assistance aimed at improving vegetation quality and reducing fire risk. A thorough description not only of the experimental site but also of the findings from the first year of irrigations at this specific location is provided in ESTRELA et al. (2009). Summing up, the Mt. Los Machos site can be divided into two parts: (a) the fog-water collection and storage area and (b) the reforestation plot itself. The former is situated 40 m above the latter, and this difference in elevation alone resulted in a water pressure of about 4 atm at the end of each irrigation line.

All the accoutrements necessary for measuring, collecting and storing fog water were set up at the top part of the experimental site, at 1025 m a.s.l. and about 80 m in a straight line from the reforestation plot. This top part is the summit of a steep mountain slope that drops approximately 300 m into a SW-to-NE valley. On the other hand, the reforestation plot covers an area of about 2500 m^2 with a SE-NE exposure and a gentle slope (<10%). Site preparation and planting took place from December 2006 to January 2007. The first plot interventions involved selective clearing (brush-chipping) using a scrub-clearing machine to clear the vegetation without altering the soil surface and the application of slash over the soil surface as a mulching layer to provide beneficial effects in terms of reducing fire risk and increasing ecosystem resilience (VALDECANTOS et al. 2009). A total of 620 one-year-old seedlings of *Pinus pinaster* and *Quercus ilex* were planted at regular intervals. Water treatments for the two species of seedlings consisted of natural precipitation as the control (C), one or two water pulses of ca. 4.5 l seedling^{-1} during the first summer after planting (W1 and W2, respectively), and rainfall exclusion (-W), the latter conducted by means of a 0.45-m^2 waterproof plastic sheet deployed over the specimen soil surface before a rainfall event was anticipated. One main hose was deployed from the fog-water storing area to the reforestation plot and connected to a manual control head (Fig. 2). Two sublines were then used to provide watering treatments W1 and W2 separately. During an irrigation pulse, water was injected 20-25 cm deep by means of microtubing connected to each of the 2 l h^{-1} emitters. Watering treatments took place on July 3rd (W2) and August 3rd (W1 and W2), 2007. In half of the specimens for each treatment, composted sewage sludge from a local composting facility was applied before planting and mixed in situ with the soil at an application rate of 22 t dry weight per hectarea.

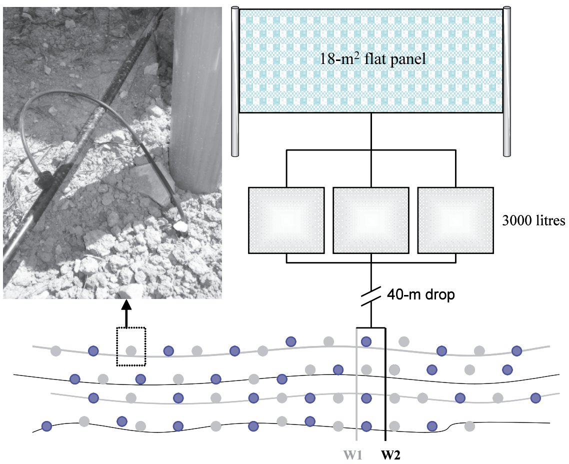

Fig. 2: Scheme of the experimental plot with the irrigation system layout. A detail of the microtube deployment is shown in the image on the left

2.2 Field data and instrumentation

At the reforestation plot, soil volumetric water content was monitored periodically by Time Domain Reflectometry (TDR) using one vertical set of two probes (0 to 30 cm depth) in 10 specimens per treatment. Soil water retention curves (drying path) of four replicates were quantified using a dewpoint hygrometer, which was adjusted with an exponential model. Rainfall on the reforestation plot was also monitored with a pluviometer at 50 cm height. Seedling survival was established for all specimens with at least one green needle or leaf. Seedling morphology (total shoot length and basal diameter) of all specimens was recorded 3 times during the first year (one month after planting and before and after the summer) and once a year during the second and third years. Basal area per hectare of both pine and holm oak was estimated using 2010 data by adding up the basal diameters of each individual seedling and assuming an initial planting density of 1000 seedlings

ha^{-1}. We calculated the net effect relative to the control as: $(Ba_1+Ba_0)/(Ba_1-Ba_0)$, where Ba_1 is the basal area of the treatment and Ba_0 is the basal area of the control. Differences in seedling survival between Species (Sp), Fertilization (F) and Water pulses (W) were evaluated using log-linear models. Seedling growth was analyzed by three-way analysis of variance with Species, Fertilization and Water pulses as fixed factors. Transformations of data were performed when necessary to ensure the validity of the assumptions of normality, linearity and homoscedasticity.

At the fog-water collection and storage area, fog-water collection rates were measured by means of a passive cylindrical fog-water collector exposed in the field together with other complementary meteorological instruments (Fig. 3, left). This instrument ensemble, fully explained in Estrela et al. (2008), consists basically of a 4-m mast supporting a wind direction and velocity sensor, a temperature and humidity probe, a rain gauge and a cylindrical fog collector. The collector is a handmade nylon string array, 26 cm in diameter and 46 cm in height, based on the ASRC (Atmospheric Science Research Center, State University of New York) collector to yield omnidirectional collection efficiency (Falconer and Falconer 1980). Additionally, a 60-cm diameter plastic tray on top of the collector carries out the function of a protective cover to avoid major rain interference (Juvik and Nullet 1995). The collected fog water volume per unit area (l/m^2) is calculated by dividing the collected volume by the effective collection surface of the collector (base diameter times height). The instrument ensemble, which registered instrumental variables every 10 minutes, was operative in the field as early as November 2006.

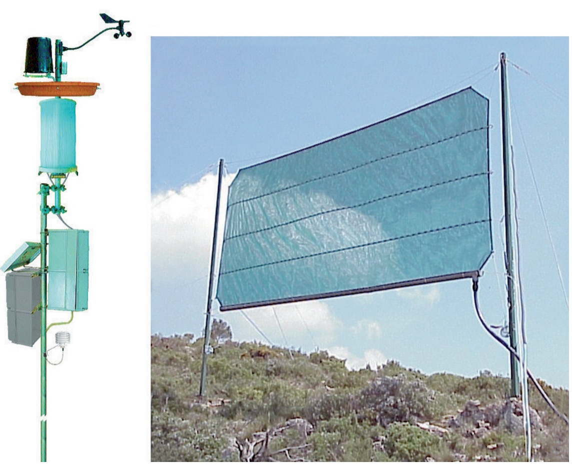

Fig. 3: Instrument ensemble containing the cylindrical collector used (left) and the 18-m² flat-panel prototype (right) for fog-water collection activities (not at the same scale)

An 18-m² flat-panel collector (Fig. 3, right), the construction of which is presented in Estrela et al. (2007), was installed at the top part of the experimental site in the vicinity of the above-described instrument ensemble. It was built with low-cost materials and used for bulk fog-water collection. With this collector, fog droplets carried by the wind are captured on a mesh, and as they become bigger they flow downwards under gravity. Water accumulates into a tilted gutter connected via a hose to three interconnected, equally levelled 1000-liter tanks to store water. The flat panel was deployed in the field in April 2007 and fixed at an orientation of 55º from North to attain maximum efficiency according to the records previously obtained from the fog instrument ensemble (Estrela et al. 2009).

2.3 Air-mass trajectories

The Air Resources Laboratory's HYbrid Single-Particle Lagrangian Integrated Trajectory (HYSPLIT) model (Draxler and Rolph 2010) is used to determine the backward and forward trajectories of air masses yielding fog water collection at the experimental site. This model provides highly valuable output on atmospheric transport and dispersion of pollutants; however, it can also be used for computing simple air parcel trajectories. HYSPLIT can be run interactively on the NOAA Air Resources Laboratory (ARL) READY (Real-time Environmental Applications and Display sYstem) website (Rolph 2010), or it can be installed on a PC and run using a graphical user interface. ARL routinely uses the National Weather Service's National Centers for Environmental Prediction (NCEP) model data and reanalysis datasets in their air quality transport and dispersion modelling calculations.

Using the HYSPLIT model, 5-day backward trajectories of air masses were calculated at the peak of each fog episode that occurred during the months of April and July 2007. These two months were selected because of their different statistical behaviour in relation to the total amount of collected fog water and the daily fog occurrence, as shown in the next section. When a continuous fog episode lasted for more than one day, as took place in April, a backward trajectory was calculated at a specified time for each of the duration days. In total, 12 and 9 trajectories were determined for April and July respectively. Due to similarities between trajectories belonging to the same month, a representative was selected for each month and subjected to a more complete analysis.

The fog episode selected for April was at its height at 20h UTC on 26/04/2007, and it concluded when dry conditions were sampled at 10h UTC on 29/04/2007; in contrast, the fog episode chosen for July peaked at 21h UTC on 14/07/2007 and ended completely at 10h UTC on the following day once dry conditions returned again. At the experimental site and for each of these four dates, the 5-day backward and forward trajectories of the air parcel at 1 m above ground level (AGL) and at 1000 m AGL provided the air mass pathways before and after the sampling by the instrumentation setup.

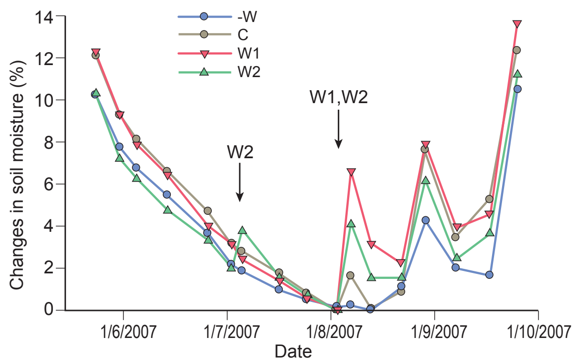

Fig. 4: Relative soil moisture levels from June to October (mean and standard error for n = 10). Each value has been normalized to the minimum value recorded in the soil within the same treatment (x_i-x_{min}) during this period. Arrows mark the timing of the water pulses

3 Results

3.1 Net effect of treatments after a three-year period

The date of the first water pulse for the W2 (W1) treatment determined a drought period of 40 (70) days with an increase in soil water content of about 26% (16%) in relation to the control treatment (Fig. 4). These differences lasted up to the occurrence of the rainy events of late August, which established a length of 75 days for the control drought period. The –W treatment reduced even further the amount of water in the soil profile (8.3%) as compared to the controls and had an associated drought period of about 90 days. Soil moisture in the rhizosphere of the seedlings reached levels as high as at early summer (14.1% in W2 and 17.5% in W1) during the days immediately after the water pulses. This effect lasted for about 3 to 5 days.

First summer seedling survival was above 70 and 80% in *P. pinaster* and *Q. ilex*, respectively, in all experimental conditions. Forty months after planting, survival was significantly lower in pine seedlings than in holm oak seedlings (61 vs. 90% on average, respectively, Tab. 2). In holm oak seedlings, survival did not decrease during the three monitoring years; in contrast, it decreased by 18% in pine seedlings. The highest survival percentages were achieved in the W2 treatment in pine (73.5%) and holm oak (100%). Fertilization did not affect survival rates, but treatments did (Tab. 3). Both watering treatments showed higher survival percentages, but no differences were found between the W1 and W2 treatments. Splitting the data by species showed that pine seedling survival was not affected either by treatment or compost application. In contrast, holm oak survival was significantly affected by water pulses ($G=17.850$, $p<0.001$) and marginally affected by compost application ($G=2.765$, $p=0.096$). Seedlings with water pulses (W1 and W2) showed 96.9% survival while the survival percentages in the –W and the control treatments were 84.2 and 81.9%, respectively. Compost application marginally reduced *Q. ilex* seedling survival, by 5% (94.3 vs. 89.0% in unfertilized and fertilized plants, respectively).

We observed a significant positive effect of compost application on the early growth of pine seedlings ($F= 5.60$ $p=0.019$), but this effect vanished in the third year after planting ($F=0.753$ $p=0.387$). Three years after planting, mean seedling height of unfertilized pines was 45.2 cm while that of fertilized ones was 49.0 cm. Similarly, basal diameter of pines that received compost was a 7.6% higher than

Tab. 2: Survival of *Pinus pinaster* and *Quercus ilex* seedlings after the first summer in the field (2007) and 40 months after planting (2010) according to water pulses and fertilization treatments

Treatment	Pinus pinaster				Quercus ilex			
	Fertilized (%)		Unfertilized (%)		Fertilized (%)		Unfertilized (%)	
	2007	2010	2007	2010	2007	2010	2007	2010
-W	70.6	52.9	73.7	52.6	84.2	84.2	84.2	84.2
C	72.2	61.1	84.2	60.5	80.0	74.3	89.2	91.9
W1	79.5	59.1	82.0	68.0	95.5	95.5	98.1	98.1
W2	87.8	73.5	81.3	60.4	95.7	95.7	98	100.0

Tab. 3: Summary of the log-linear analyses of seedling survival for the 3-year period. Partitioned likelihood ratio statistic (G) and p values of the log-linear analysis

Source of variation	df	G	p
Sp	1	77.83	0.000
F	1	0.30	0.582
W	1	10.61	0.014
Sp x F	3	2.22	0.136
Sp x W	3	9.60	0.022
F x W	3	2.64	0.450
Sp x F x W	3	0.41	0.937

Sp = species, F = fertilization, and W= water pulses.

that of the controls (7.1 vs. 6.6 mm, respectively). On the other hand, in holm oak seedlings, the fertilization with composted sewage sludge produced a slight negative effect on growth (F=6.31 p=0.013), reducing seedling mean basal diameter from 5.7 to 5.3 mm. It appears that water pulses did not change the seedling growth pattern in the short and medium term. However, the tallest pines three years after planting were those receiving two water pulses (W2) while the shortest pines were those with rainfall exclusion (-W) (50.0 and 42.1 cm, respectively). Surprisingly, oak seedlings planted in the rainfall exclusion treatment tended to grow more than control seedlings while watering treatments presented intermediate values (32.8, 33.2, 34.9 and 36.2 cm in C, W2, W1 and –W, respectively). Basal area per hectare integrates survival and growth data and showed a synergistic net effect between water and compost application in *P. pinaster.* In holm oak, net effects were similar for both water pulse and fertilization factors, without significant interactions (Fig. 5).

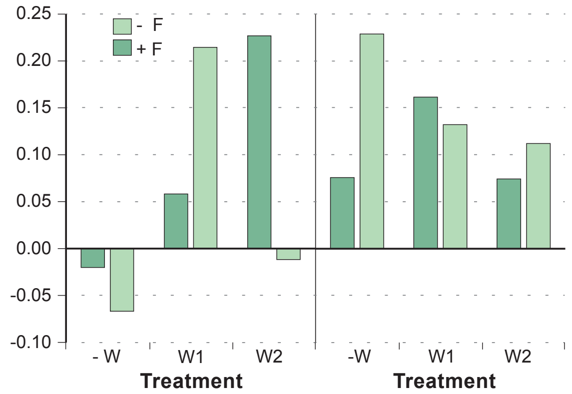

Fig. 5: Net effect of treatments on basal area of *P. pinaster* (left) and *Q. ilex* (right) seedlings in relation to fertilization and water pulses treatments 40 months after planting. Values range between -1 and 1 indicating positive (> 0) or negative (<0) effect of the treatments as compared to the control (y=0)

3.2 Monthly fog-water collection

Figure 6 shows the monthly fog collection and precipitation rates, i.e. the ratio of water collected volumes to the length in days of available data for each of the months in the 3-year period. For 2007 (2008, 2009), the outcome for the annual rate of fog collection was 3.3 (4.1, 2.1) l/m2/day, whereas the annual precipitation totalled 536 (822, 607) mm. In general, the wettest of the three study years with respect to both fog collection and rainfall was 2008. However, it is interesting to note that 2009, although yielding less fog collection than 2007, provided a larger precipitation amount. Monthly inter-annual variability for both fog collection and rainfall was large all year long, particularly during the spring and autumn seasons. Summer and early autumn are probably the periods with the lowest inter-annual variability. The largest monthly yields in both precipitation and fog occurred during September and October; it is interesting to contrast this with the results for the month of November, when depletion in both yields was consistently observed during the 3-year study period. As the figure shows, fog collection does not stop during summer, although rainfall is drastically reduced.

3.3 Wind and fog-occurrence statistics for a three-year period

Statistical distributions of the different wind frequencies at the experimental site are represented by wind roses. The wind rose of the entire 3-year wind data set taken by the instrument ensemble is given at the top of figure 7, the "all data" wind rose. The inter-annual variability for the period considered is small, about 3.3% for the wind direction and 1.7% for the wind velocity, which indicates year-to-year repeatability of wind patterns. The most frequent winds are distributed into two main components and a third secondary one: a marked component peaking between the NE and ENE directions, a strong component in the WNW direction, and an interface towards the third component peaking in the SSW direction.

The above wind patterns can be disaggregated by examining the winds bearing fog, on the one hand, and the winds associated with dry conditions,

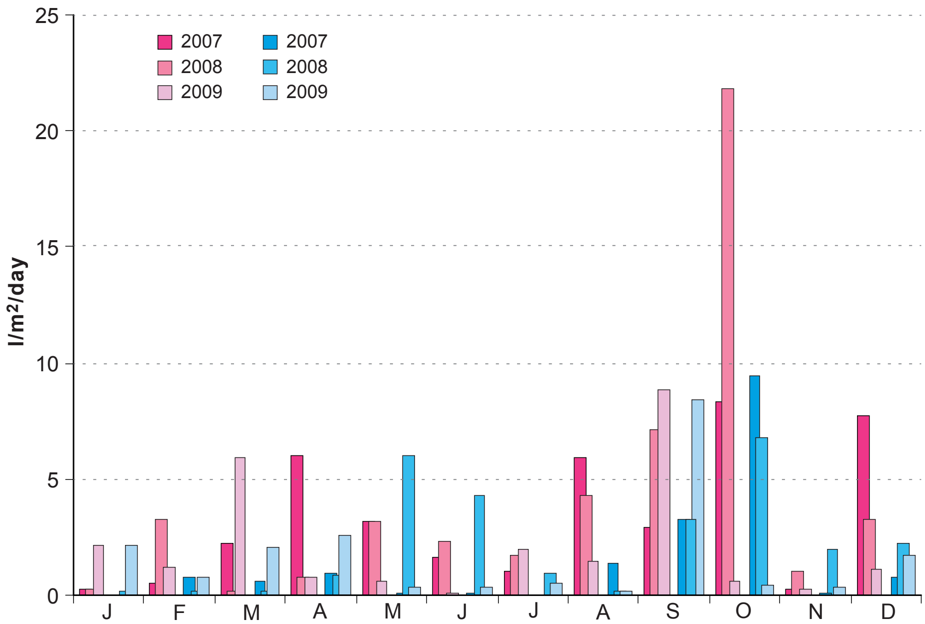

Fig. 6: Monthly fog collection (reddish patterns) and precipitation (bluish patterns) rates for the 3-year study period

on the other hand, i.e., the moist and dry extremes for all cases. The wind rose represented in the middle of figure 7, the "fog occurrence" wind rose, is constructed from the "all data" wind rose by selecting the winds with fog occurrence, about 11% of the total winds. The bottom figure in figure 7 is for the "low relative humidity" wind rose, where wind extraction from the "all data" wind rose satisfies the condition of a relative humidity under 40%, about 16% of the total winds. Winds that do not satisfy either of the two extremes are a mixture of these two components. The "fog occurrence" wind rose shows a single large component which stretches between the NE and the ENE. This direction is precisely the valley orientation and also the shortest way to the coastline. The relative inter-annual variability of the winds bearing fog is a bit larger than in the "all data" wind rose: about 11% for the wind direction and 9% for the wind velocity. In contrast, the "low relative humidity" wind rose shows a broad component stretching from the NW to the S and peaking at the SSW direction and less intensively at the W direction. A tiny component in the ENE direction is also seen. The relative inter-annual variability of the winds under dry conditions is a bit smaller: about 6.5% for the wind direction and 8.5% for the wind velocity.

The ratio of one-hour episodes delivering any amount of fog water to the total amount of hours in the 3-year period was 14%. Figure 8 shows the hourly percentage of fog collection occurrence disaggregated by month and by time of day. A regular daily cycle of fog occurrence is clearly observed; it is slight or inexistent for the period from November to June, but prominent from July to October. During the summer months and the first half of autumn, fog occurs most frequently during the early morning and late evening, at it is almost completely inhibited around midday.

3.4 Fog air-mass trajectories

Five-day backward and forward trajectories at 1 and 1000 m AGL over the experimental site are given for 26/04/2007 at 20h UTC and 29/04/2007 at 10h UTC in figure 9, and for 14/07/2007 at 21h UTC and 15/07/2007 at 10h UTC in figure 10. On 26 April 2007, the air-mass origin at maximum fog collection was entirely from the Mediterranean Sea, straight from the Tyrrhenian Sea at surface level into the Valencia region where orographic lifting took place. After crossing over the experimental area and generating fog collection, the air-mass continued on its way until it reached the central part of the Iberian Peninsula where it changed direction to head backwards. When the fog episode concluded, on the morning of 29 April 2007 (Fig. 9), the superficial fetch over the Mediterranean Sea for the backward trajectory was even larger than on the previous days; however, the air-mass penetrated into the northern part of the Valencia region and turned back head-

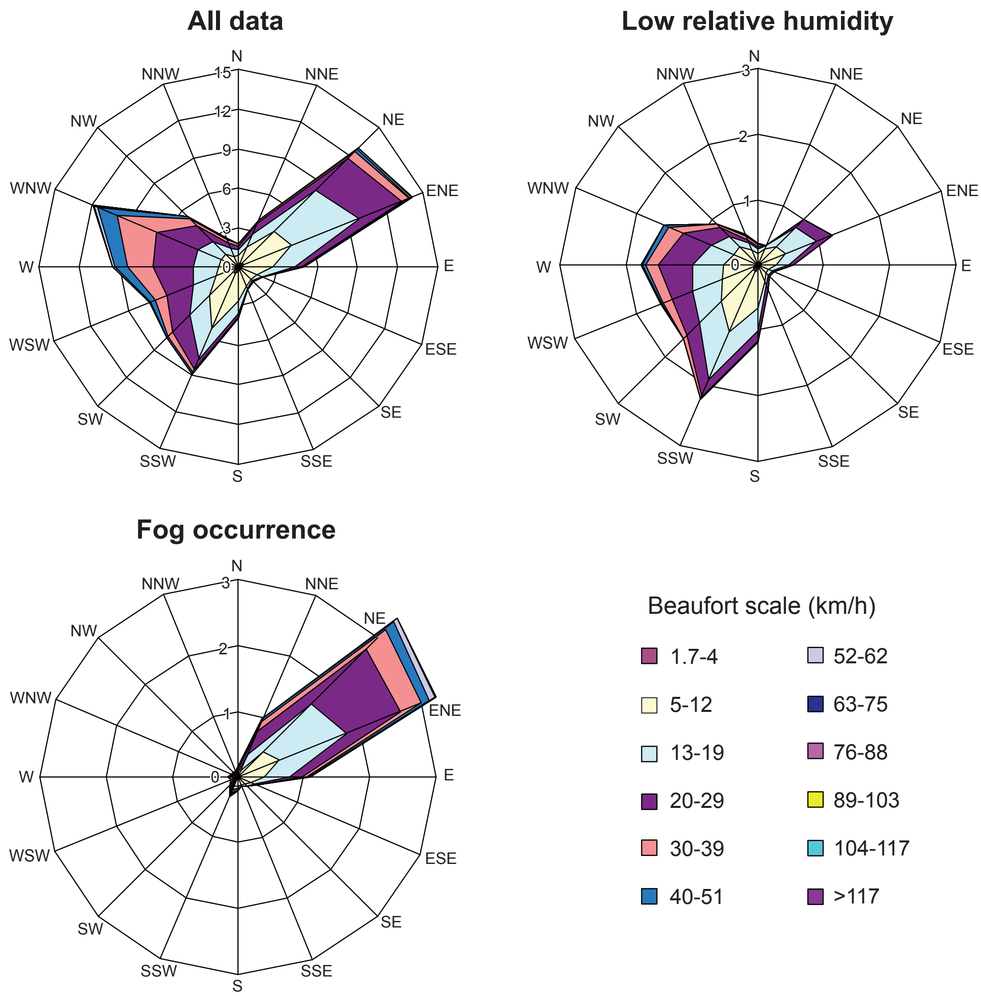

Fig. 7: 3-year wind roses for the entire set of wind data (top-left), frequency of wind with simultaneous fog collection occurrence (bottom) and selection of winds under low (<40%) relative humidity conditions (top-right). Data values are distributed into 16 wind direction bins and a Beaufort wind velocity scale. Concentric circles correspond to wind frequencies relative to the entire set of wind data

ing East when crossing over the experimental site. At this point, the air mass was descending, fog formation was depleted and the wind direction at the site was moving away from the moist wind component (Fig. 7) into the dry wind component. The 1000 m AGL trajectory was also in a descending movement after its pass over the experimental site, indicating either the dissipation of cloudiness or its migration to northern regions. A representation of the data taken by the instrument ensemble at the experimental site during the April fog episode is provided in figure 11. Fog water collection took place mainly at the beginning of the episode, before 27/04/2007. During the whole length of the episode, the fog water volume totalled 31 l/m^2, in contrast to the measured precipitation, which was 3 l/m^2. For comparison purposes, Figure 9 shows that the rainfall registered at a lowland meteorological station (Ayora municipality) located 13 km away from the study site totalled 15 l/m^2 for the period in question. This figure also shows the measured wind direction to emphasize its change from before the onset of the episode to the end of the episode.

The fog episode selected for July was at its maximum at 21h UTC on 14 July 2007 (Fig. 10). 1-m AGL air masses came in a descending movement from the Bay of Biscay until reaching the surface of the Balearic Sea, where they headed westwards onto the coasts of the Valencia region. 1000-m AGL air masses followed a similar pattern, except that they did not reach the sea surface as they stayed at around 500 m a.s.l. The 1-m AGL air masses cooled down and took

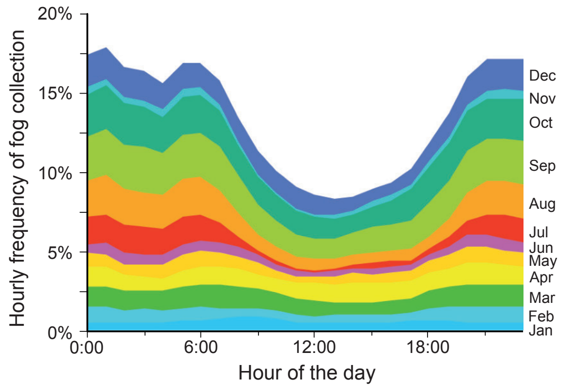

Fig. 8: Hourly percentage of fog collection occurrence disaggregated by month and hour of day for the 3-year study period. Each of the patterns represents the monthly contribution to the total annual occurrence

up moisture on their way over the sea surface until the topography provoked their lifting. The path associated with the 1 (1000) m AGL air mass resulted in an ENE (SE) wind direction at the experimental site, heading northwards as the air masses crossed over the site and progressed into the Iberian Peninsula. When the fog episode ended at 10h UTC on 15 July 2007, the paths followed by the air masses showed a pattern similar to the one found when the episode was at its maximum. Thus, the explanation of the onset and end of the fog episode requires another approach. A representation of the data taken by the instrument ensemble during the July fog episode is given in figure 12. Fog water collection started abruptly and gradually decreased until the conclusion of the episode, yielding 7 l/m^2 in total. The only meteorological variable that changed in the process, besides (logically) the relative humidity, was the air temperature, as shown in the figure. Air temperature started to deplete before the onset of the fog episode and rose again on the morning of the next day, right at the time when the episode concluded.

In order to understand the fog formation and cessation in the above case episodes, a synoptic analysis was carried out using both the NCEP reanalysis charts at 500 hPa and the surface pressure charts, as found in Wetterzentrale (http://www.wetterzentrale.de/). For the case episode of April (Fig. 13), high pressures in central Europe created a blocking mechanism over the Netherlands, and a relative disturbance slid from the North Atlantic

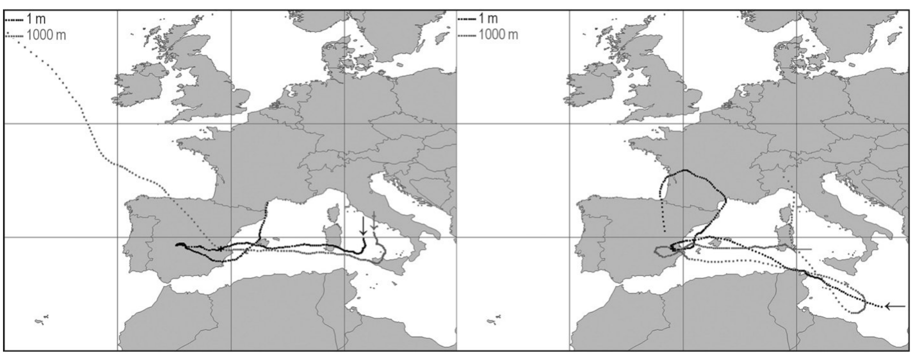

Fig. 9: 120-h backward and forward trajectories at 1-m (black points) and 1000-m (grey points) AGL at the experimental site for the fog episode at 20h UTC on 26/04/2007 (left) and its conclusion at 10h UTC on 29/04/2007 (right). Arrows indicate the starting point for each trajectory

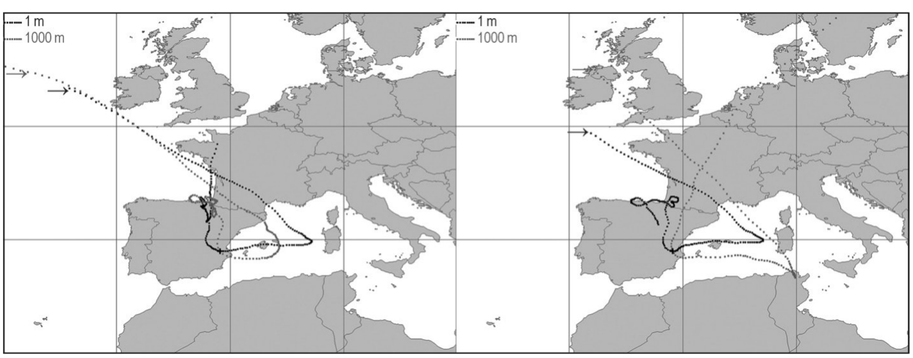

Fig. 10: 120-h backward and forward trajectories at 1-m (black points) and 1000-m (grey points) AGL at the experimental site for the fog episode at 21h UTC on 14/07/2007 (left) and its conclusion at 10h UTC on 15/07/2007 (right). Arrows indicate the starting point for each trajectory

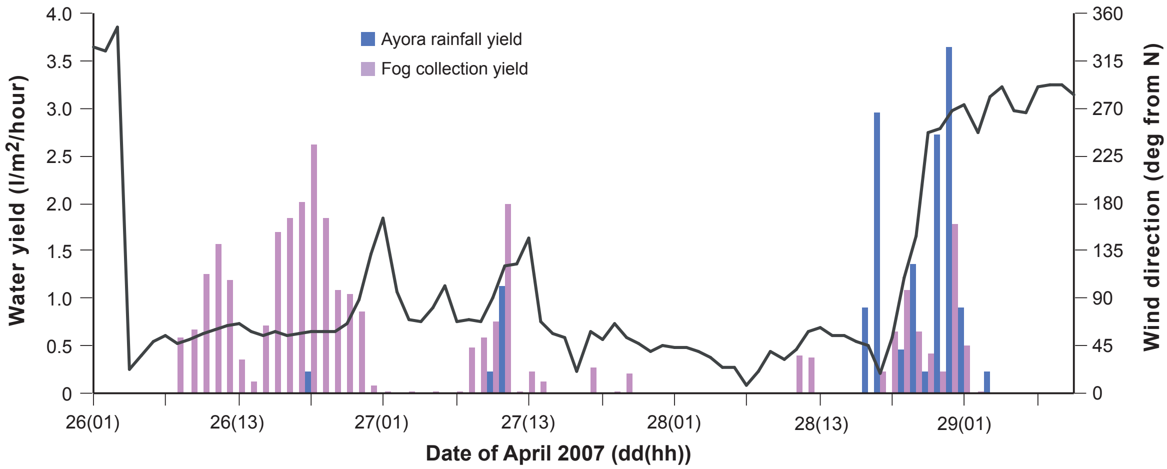

Fig. 11: Time series of hourly yields of fog water and hourly averages of wind direction at the experimental site during the case episode of April 2007. The hourly rainfall measured at Ayora, a lowland area at a distance of 13 km, is also provided

onto the Iberian Peninsula. This relative low promoted a slight instability at high levels resulting in low and medium cloud development with occasional and small precipitations. A long distance flow across the Mediterranean Sea was sustained by the central Europe anticyclone bringing moist air towards the Iberian Peninsula. The conclusion of the synoptic situation stems from the entrance of a western flow bringing dry and cold air into the Iberian Peninsula.

For the case episode of July (Fig. 14), the synoptic chart was controlled by a trough over the North Atlantic with a warm front maintained over the Iberian Peninsula and a subsidence produced by high pressures over the Mediterranean Sea. The subsidence promoted the establishment of gentle sea breezes on the Valencia region which were maintained all day, even at night. Above 1500 m, SW warm dry air penetrated over the eastern half of the Iberian Peninsula defining the limit of the atmospheric boundary layer through a thermal inversion and the edge for the warm front of the Atlantic trough. A vertical wedge shape characterized the inland incursion of the humid sea breezes from the Mediterranean Sea. During the daytime and due to solar heating and topography, the lifting condensation level (LCL), which defines the height of the cloud base, could be around 900 hPa for an unbroken boundary layer. Due to the presence of a strong thermal inversion, when solar heating was removed at night-time, the LCL could drop to 950 hPa or even further, easily reaching mountain tops such as the experimental site at Mt. Los Machos. Mechanical lift makes the air mass temperature drop according to the adiabatic rate until the dew point is reached and condensation begins to form rendering clouds and fogs eventually.

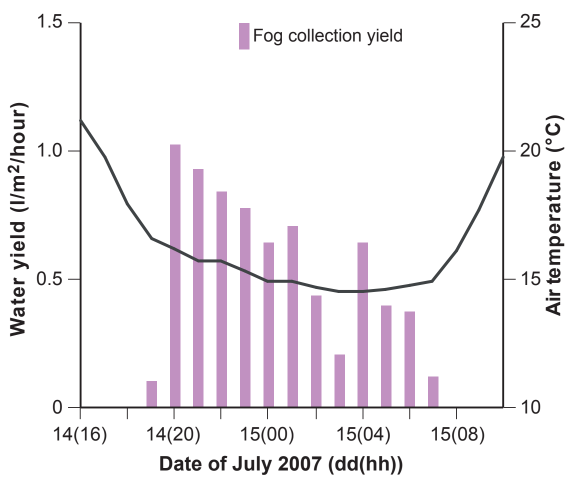

Fig. 12: Time series of hourly yields of fog water and hourly averages of air temperature at the experimental site during the case episode of July 2007

4 Discussion

Although the afforestation period could be considered mild in pluviometric terms, the data on seedling survival confirms that the application of small water pulses can significantly increase reforestation success. Small water inputs applied deeply by drip irrigation may be sufficient to substantially decrease seedling mortality (Padilla and Pugnaire 2009). Drip irrigation favours long-term water availability, minimizes the abundance of competing vegetation and avoids the presence of herbivores that are attracted by surface water. Furthermore, it promotes water

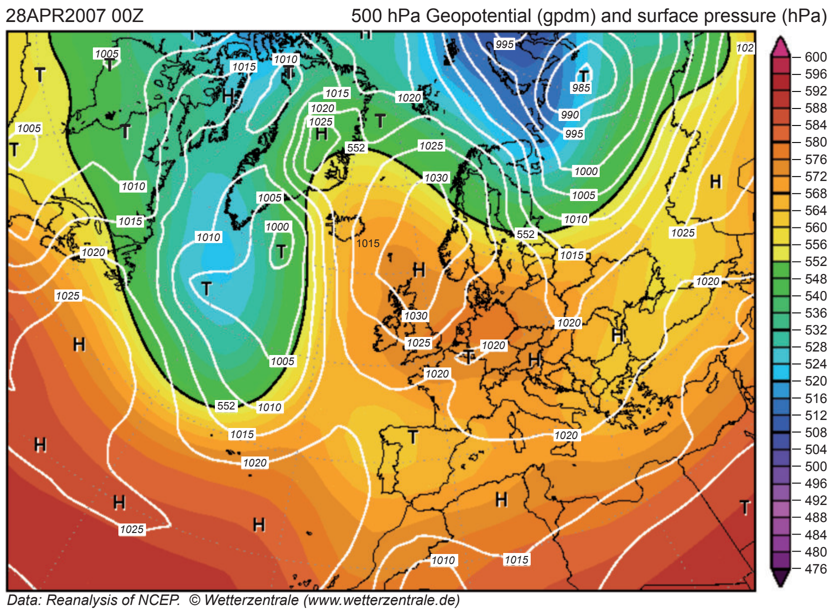

Fig. 13: NCEP/NCAR 00 UTC reanalysis 500 hPa and surface pressure synoptic chart for 28/04/2007, as found in Wetterzentrale (http://www.wetterzentrale.de/)

infiltration and storage in deeper soil horizons where roots show higher activity during the first stages of seedling development. The application of the same amount of water at the surface of the planting hole would saturate no more than 10-15 cm of the soil profile subjected to high evaporative demand.

The high seedling survival, mainly of *Q. ilex*, as compared with other field experiments in the same area (Pausas et al. 2004; Valdecantos et al. 2006) could also be explained by the regular late-evening and morning fog episodes that occurred during summer. In dry Mediterranean areas, these episodes can provide a substantial percentage of the water absorbed by roots during summer droughts (Corbin et al. 2005) and also lower the evapotranspiration rates that affect the water and energy exchange at the atmosphere–land interface (Katata et al. 2010). The significance of nutrient availability and water pulses is contrasted in the two studied species. This result may be related to the contrasting ecological features and strategies of *P. pinaster* and *Q. ilex*. For example, the small increment in soil humidity provided by microcatchments increased *Q. ilex* seedling survival in a degraded dryland, while it mainly affected *P. halepensis* growth rate during the 36 months after planting (Fuentes et al. 2004). Early successional species, like *P. pinaster*, tend to keep foliar concentrations of the most limiting nutrient at relatively constant levels when its availability increases, using the extra nutrient inputs to increase growth (Bazzaz 1979). In contrast, late-successional species, like *Q. ilex*, have a conservative resource-use strategy (Valladares et al. 2000) and allocate supplemental nutrient inputs to belowground storage organs (Rapp et al. 1999) showing less plasticity in aboveground morphology and physiology. This species is stimulated to a higher extent by water than by nutrient availability (Sanz-Pérez et al. 2007; Rey-Benayas and Camacho 2004); however, the growth pattern of *Q. ilex* did not change with either water or nutrient availability while *P. pinaster* showed enhanced growth rates with the application of composted biosolid during the first year, 2007. In this sense, early-successional species show higher ecological plasticity as their growth responds to increases in both resources (Canham et al. 1996) although these effects commonly disappear with time once the root system is well established.

With an annual fog water rate of 3.2 l/m^2/day for the 3-year study period, the experimental site can be classified as having a moderate-to-low potential for fog water collection. High-ranking sites can yield as much as 9-10 l/m^2/day depending on the characteristics of the year (Marzol 2005). At our site, recurrent fog episodes from July to September led to a minimum rate of, at least, 1 l/m^2/day for the summer period. The hourly periodicity of these summer events was centred during night-time, between 20 UTC and 07 UTC the next morning. Synoptic chart examination explained the fog formation in terms of the mechanical lifting of moist air and its trapping aloft by the thermal inversion defining the upper limit of the boundary layer. The drop in air temperature (Fig. 12)

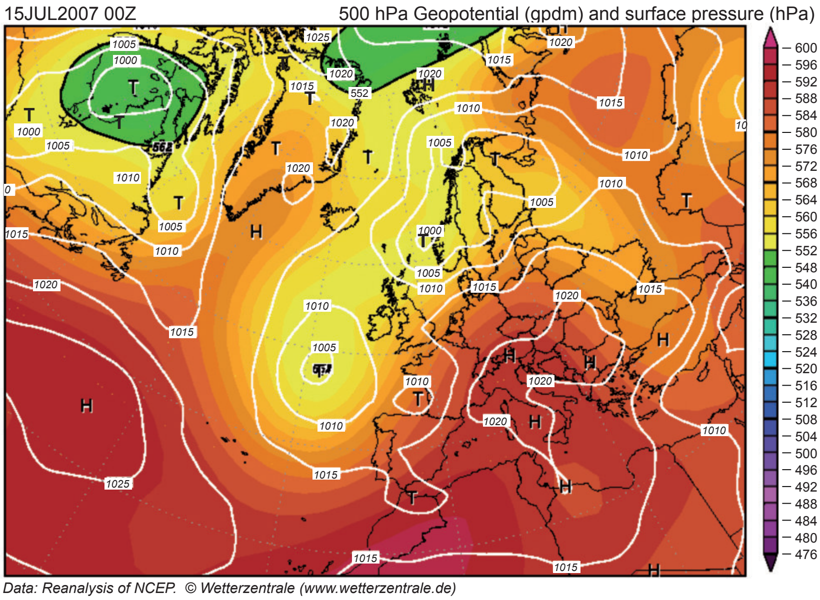

Fig. 14: NCEP/NCAR 00 UTC reanalysis 500 hPa and surface pressure synoptic chart for 15/07/2007, as found in Wetterzentrale (http://www.wetterzentrale.de/)

revealed the adiabatic cooling of the air mass in its ascending movement across the mountain slopes. Well-established and night-persistent sea breezes were also necessary. Backward trajectory analysis provided no additional information for this type of episode. In contrast, outside of the summer months, the hourly periodicity of the fog collection vanished. Fog formation during the non-summer period was due to the mechanical lift caused by a nearby relative disturbance or trough, and it was independent of time. Moist air and Mediterranean flows were also necessary to create the conditions for fog formation. The episode conclusion came when the disturbance moved away or passed over the site, causing the winds to change and bring drier conditions typical of subsidence air.

5 Conclusions

It is likely that the climatic conditions of the planting year, including the number of fog episodes, were not stressful enough to generate strong water limitation in the seedlings. However, small water pulses during the first summer in the field promoted short and medium term seedling survival, as well as higher initial growth of pines. The application of small water pulses to reduce the length of the drought period by splitting it into several less stressful intervals is an interesting option for restoring burned and degraded areas more efficiently. It is expected that the more stressful the environmental conditions are, the more efficient the water pulses will be. The continuous in situ collection of alternative water inputs throughout the year implies a diversification of the main objectives of restoration. The lack of effects in holm oak seedlings highlights the relevance of matching target species and field treatments. Mountainous sites in the western Mediterranean region are prone to fog formation when the right atmospheric conditions are combined with maritime air masses. There is a favoured direction for winds that bear fog at the experimental site due to local topography and the specific trajectories of the maritime air masses. In addition, daily patterns of fog collection are observed for summer and early autumn; they can be explained in terms of the mechanical lifting of sea breeze air under thermal inversion conditions. Conversely, fogs forming outside of summer are caused by frontal systems and show time-independent patterns.

Acknowledgements

This research was supported by the Ministerio de Educación y Ciencia, contract numbers CGL2010-16364/CLI, CGL2005-03386/CLI, CGL2007-65774/CLI, CGL2008-04550/CLI, the CONSOLIDER-INGENIO 2010 program, GRACCIE project CSD2007-00067, and the Ministerio de Medio Ambiente, RECUVES project, contract number 077/RN08/04.1. We especially want to thank Mr J. Miró,

F. García and Ms M. J. Barberá for their technical assistance. We thank NCEP/NCAR for supplying data. The authors gratefully acknowledge the NOAA Air Resources Laboratory (ARL) for providing the HYSPLIT transport and dispersion model and/or READY website. The manuscript was revised by J. Scheiding. Instituto Universitario CEAM-UMH is supported by the Generalitat Valenciana and Fundación Bancaja.

References

Allen, E. (1995): Restoration ecology: limits and possibilities in arid and semiarid lands. In: Proceedings of the Wildland Shrub and Arid Land Restoration Symposium, A. Forest Service INT-GTR-315. Washington DC, 7–15.

Baeza, M. J.; Raventos, J.; Escarré, A. and Vallejo, V. R. (2006): Fire risk and vegetation structural dynamics in Mediterranean shrubland. In: Plant Ecology 187, 189–201. DOI: 10.1007/s11258-005-3448-4

Baeza, M. J.; Valdecantos, A.; Alloza, J. A. and Vallejo, V. R. (2007): Human disturbance and environmental factors as drivers of long-term post-fire regeneration patterns in Mediterranean forests. In: Journal of Vegetation Science 18, 243–252. DOI: 10.1111/j.1654-1103.2007.tb02535.x

Bainbridge, D. A. (2002): Alternative irrigation systems for arid land restoration. In: Ecological Restoration 20, 23–30.

Bazzaz, F. A. (1979): Physiological ecology of plant succession. In: Annual Review of Ecology and Systematics 10, 351–371. DOI: 10.1146/annurev.es.10.110179.002031

Canham, C. D.; Berkowitz, A. R.; Kelly, V. R.; Lovett, G. M.; Ollinger, S. V. and Schnurr, J. (1996): Biomass allocation and multiple resource limitation in tree seedlings. In: Canadian Journal of Forest Research 26, 1521–1530. DOI: 10.1139/x26-171

Corbin, J.; Thomsen, M. A.; Dawson, T. E. and d'Antonio, C. M. (2005): Summer water use by California coastal prairie grasses: fog, drought, and community composition. In: Oecologia 145, 511–521. DOI: 10.1007/s00442-005-0152-y

Draxler, R. R. and Rolph, G. D. (2010): HYSPLIT (HYbrid Single-Particle Lagrangian Integrated Trajectory) Model – NOAA ARL READY Website. NOAA Air Resources Laboratory, Silver Spring. http://ready.arl.noaa.gov/HYSPLIT.php

Estrela, M. J.; Valiente, J. A.; Corell, D. and Millán, M. M. (2004): Fog collection in a region of the western Mediterranean basin: evaluation of the use of fog water for the restoration of wildfire burnt areas. In: Proceedings of the Third Int Conf on Fog, Fog Collection and Dew, Cape Town, South Africa, M2.

Estrela, M. J.; Valiente, J. A.; Corell, D. and Fuentes, D. (2007): Collection of fog water for the restoration of degraded forest areas in a western Mediterranean basin region. Preliminary results. In: Proceedings of the Fourth Int. Conf. on Fog, Fog Collection and Dew. La Serena, Chile, 113–116.

Estrela, M. J.; Valiente, J. A.; Corell, D. and Millán, M. M. (2008): Fog collection in the western Mediterranean basin (Valencia region, Spain). In: Atmospheric Research 87, 324–337. DOI: 10.1016/j.atmosres.2007.11.013

Estrela, M. J.; Valiente, J. A.; Corell, D.; Fuentes, D. and Valdecantos, A. (2009): Prospective use of collected fog water in the restoration of degraded burned areas under dry Mediterranean conditions. In: Agricultural and Forest Meteorology 149, 1896–1906. DOI: 10.1016/j.agrformet.2009.06.016

Falconer, R. E. and Falconer, P. D. (1980): Determination of cloud water acidity at a mountain observatory in the Adirondack Mountains of New York State. In: Journal of Geophysical Research 85, 7465–7470. DOI: 10.1029/JC085iC12p07465

Fuentes, D.; Valdecantos, A. and Vallejo, V. R. (2004): Plantación de *Pinus halepensis Mill.* y *Quercus ilex subsp. ballota (Desf) Samp.* en condiciones Mediterráneas secas utilizando microcuencas. In: Cuadernos de la SECF 14, 157–161.

Juvik, J. O. and Nullet, D. (1995): Comments on 'A proposed standard fog collector for use in high elevation regions'. In: Journal of Applied Meteorology 34, 2108–2110. DOI: 10.1175/1520-0450(1995)034<2108:COPS-FC>2.0.CO;2

Katata, G.; Nagai, H.; Kajino, M.; Ueda, H. and Hozumi, Y. (2010): Numerical study of fog deposition on vegetation for atmosphere-land interactions in semi-arid and arid regions. In: Agricultural and Forest Meteorology 150, 340–353. DOI: 10.1016/j.agrformet.2009.11.016

Lovich, J. E. and Bainbridge, D. (1999): Anthropogenic degradation of the southern California desert ecosystem and prospects for natural recovery and restoration. In: Environmental Management 24, 309–326. DOI: 10.1007/s002679900235

Marzol, M. V. (2005): La captación del agua de niebla en la isla de Tenerife. In: Publicación 333, investigación 61, Caja General de Ahorros de Canarias. Tenerife, Canarias.

Millán, M. M.; Estrela, M. J. and Vallejo, R. (1998): Evaluation of the hydrological inputs in the Mediterranean basin. In: Proceedings of the First Int. Conf. on Fog and Fog Collection. Vancouver, Canada, 281–284.

Padilla, F. M. and Pugnaire, F. I. (2009): Species identity and water availability determine establishment success under the canopy of *Retama sphaerocarpa* shrubs in a dry environment. In: Restoration Ecology 17, 900–907. DOI: 10.1111/j.1526-100X.2008.00460.x

Pausas, J. G.; Bladé , C.; Valdecantos, A.; Seva, J. P.; Fuentes, D.; Alloza, J. A.; Vilagrosa, A.; Bautista, S.; Cortina, J. and Vallejo, R. (2004): Pines and oaks in the restoration of Mediterranean landscapes: new perspectives for an old practice. In: Plant Ecology 171, 209–220. DOI: 10.1023/B:VEGE.0000029381.63336.20

Peñarrocha, D. (1994): Precipitaciones: volúmenes y distribución espacial. In: Pérez-Cueva, A. (ed.): Atlas Climático de la Comunidad Valenciana (1961–1990). Valencia, 86–89.

Rapp, M.; Santa Regina, I.; Rico, M. and Gallego, H. A. (1999): Biomass, nutrient content, litterfall and nutrient return to the soil in Mediterranean oak forests. In: Forest Ecology and Managament 119, 39–49. DOI: 10.1016/S0378-1127(98)00508-8

Rey-Benayas, J. M. and Camacho, A. (2004): Performance of *Quercus ilex* saplings planted in abandoned Mediterranean cropland after long-term interruption of their management. In: Forest Ecology and Management 194, 223–233. DOI: 10.1016/j.foreco.2004.02.035

Rivas-Martinez, S. (1987): Mapa de series de vegetación de España 1:400000 y memoria. In: Serie Técnica. Madrid.

Rolph, G. D. (2010): Real-time Environmental Applications and Display sYstem (READY). NOAA Air Resources Laboratory, Silver Spring. http://ready.arl.noaa.gov

Sanz-Pérez, V.; Castro, P. and Valladares, F. (2007): Growth versus storage: responses of Mediterranean oak seedlings to changes in nutrient and water availabilities. In: Annals of Forest Science 64, 201–210. DOI: 10.1051/forest:2006104

Schemenauer, R. S. and Cereceda, P. (1994): A proposed standard fog collector for use in high-elevation regions. In: Journal of Applied Meteorology 33, 1313-1322. DOI: 10.1175/1520-0450(1994)033<1313:APSFCF>2.0.CO;2

Valdecantos, A.; Cortina, J. and Vallejo, V. R. (2006): Nutrient status and field performance of tree seedlings planted in Mediterranean degraded areas. In: Annals of Forest Science 63, 249–256. DOI: 10.1051/forest:2006003

Valdecantos, A.; Baeza, M. J. and Vallejo, V. R. (2009): Vegetation management for promoting ecosystem resilience in fire-prone Mediterranean shrublands. In: Restoration Ecology 17, 414–421. DOI: 10.1111/j.1526-100X.2008.00401.x

Valiente, J. A.; Estrela, M. J. and Corell, D. (2007): Fog Collection Network in the Valencia Region (Western Mediterranean Basin). In: Proceedings of the Fourth Int. Conf. on Fog, Fog Collection and Dew. La Serena, Chile, 399–402.

Valladares, F.; Martínez-Ferri, E.; Balaguer, L.; Perez-Corona, E. and Manrique, E. (2000): Low leaf-level response to light and nutrients in Mediterranean evergreen oaks: a conservative resource-use strategy? In: New Phytologist 148, 79–91.

Vallejo, V. R.; Serrasolses, I.; Cortina, J.; Seva, J. P.; Valdecantos, A. and Vilagrosa, A. (2000): Restoration strategies and actions in Mediterranean degraded lands. In: Enne, G.; Zanolla, C. and Peter, D. (eds.): Desertification in Europe: mitigation strategies, land-use planning. European Communities EUR 19390. Brussels, 221–233.

Villegas, J. C.; Tobón, C. and Breshears, D. D. (2008): Fog interception by non-vascular epiphytes in tropical montane cloud forests: dependencies on gauge type and meteorological conditions. In: Hydrological Processes 22, 2484–2492. DOI: 10.1002/hyp.6844

Authors

Dr. José A. Valiente
David Corell
Unidad Mixta CEAM-UVEG
Instituto Universitario Centro de Estudios Ambientales del Mediterráneo CEAM-UMH
Parque Tecnológico
Calle Charles R. Darwin 14
46980 Paterna
Spain
josean@ceam.es
dacocus@ceam.es

Dr. María J. Estrela
Unidad Mixta CEAM-UVEG
Departament de Geografia de la Universitat de València (UVEG)
Avda. Blasco Ibañez 28
46010 Valencia
Spain
majoesna@uv.es

Dr. David Fuentes
Dr. Alejandro Valdecantos
Dr. Manuel J. Baeza
Unidad Mixta CEAM-UA
Fundación de la Comunidad Valenciana
Centro de Estudios Ambientales del Mediterráneo (CEAM)
Parque Tecnológico
Calle Charles R. Darwin 14
46980 Paterna
Spain
david.fuentes@ua.es
a.valdecantos@ua.es
jaime.baeza@ua.es